STED microscopy with continuous wave beams

Katrin I Willig[1,2], Benjamin Harke[1,2], Rebecca Medda[1] & Stefan W Hell[1]

We report stimulated emission depletion (STED) fluorescence microscopy with continuous wave (CW) laser beams. Lateral fluorescence confinement from the scanning focal spot delivered a resolution of 29–60 nm in the focal plane, corresponding to a 5–8-fold improvement over the diffraction barrier. Axial spot confinement increased the axial resolution by 3.5-fold. We observed three-dimensional (3D) subdiffraction resolution in 3D image stacks. Viable for fluorophores with low triplet yield, the use of CW light sources greatly simplifies the implementation of this concept of far-field fluorescence nanoscopy.

Since the 19th century, the resolution of any lens-based (far-field) microscope has been curtailed by diffraction to $\lambda/(2\mathrm{NA}) > 200$ nm, with λ denoting the light's wavelength and NA, the numerical aperture of the lens[1]. The emergence of STED microscopy[2–5] in the last decade showed that, at least for fluorescence imaging, these limits can be overcome. In brief, a STED microscope creates focal regions of molecular excitation that are much smaller than the diffraction limit. Typically, the diffraction spot of the excitation beam of a scanning microscope is overlapped with a doughnut-shaped spot of longer wavelength $\lambda_{\mathrm{STED}} > \lambda_{\mathrm{exc}}$ to instantly de-excite markers from their fluorescent state S_1 to the ground state S_0 by stimulated emission[2,3,6]. Thus, effective molecular excitation is confined to the doughnut center. The higher the intensity of the doughnut, the narrower the spot becomes from which fluorescence may originate. Scanning a sharpened spot through the specimen renders images with subdiffraction resolution.

Until now, STED microscopy has relied on tightly synchronized trains of pulses: excitation pulses of <80 ps duration are typically followed by 250-ps pulses for STED[2,3,5]. Matching λ_{STED} to the emission spectrum of the dye even called for tunable pulsed lasers, such as a mode-locked Ti:sapphire laser emitting in the near-infrared. Extending STED to the visible spectrum requires conversion of the pulses to shorter λ_{STED} by complex nonlinear optics[4,5,7]. Complexity is augmented by the fact that the 200-fs pulses originating from the laser system have to be stretched by 1,000-fold using optical fibers or gratings[5]. Finally, the STED pulses require synchronization with their excitation counterparts. Although these matters are routine in laser spectroscopy, the apparent need for sophisticated pulse preparation hampered the wider use of this concept. Here we show that STED microscopy can be implemented with CW lasers, making the use of pulses obsolete in many cases.

The principles of CW STED are readily explained. CW excitation at a rate k_{exc} populates S_1 with probability $N_1 = k_{\mathrm{exc}} / (k_{\mathrm{exc}} + k_{\mathrm{fl}}) < 1$; the fluorescence decay rate $k_{\mathrm{fl}} = 1/\tau_{\mathrm{fl}}$ is given by the inverse of the S_1 lifetime τ_{fl}[8]. The addition of a CW STED beam of intensity I just adds another decay rate $k_{\mathrm{STED}} = \sigma I$, yielding $N_1 = k_{\mathrm{exc}} / (k_{\mathrm{exc}} + k_{\mathrm{fl}} + k_{\mathrm{STED}}) < 1$. σ denotes the molecular cross-section for stimulated emission, whereas I is the intensity of the STED beam in photons per area and per second. Adjusting $k_{\mathrm{STED}} > k_{\mathrm{fl}} > k_{\mathrm{exc}}$ renders STED predominant, which is the case for $I > (\sigma\tau_{\mathrm{fl}})^{-1} \equiv I_s$. The CW power required to produce I_s is given by $P_s = A \times hc / (\lambda_{\mathrm{STED}}\, \sigma\tau_{\mathrm{fl}})$, with c, h and A denoting the speed of light, Planck's constant and doughnut area, respectively. At $\lambda_{\mathrm{STED}} = 650$ nm, an oil immersion lens of NA = 1.4 yields $A \approx 3 \times 10^{-9}$ cm^2 as doughnut

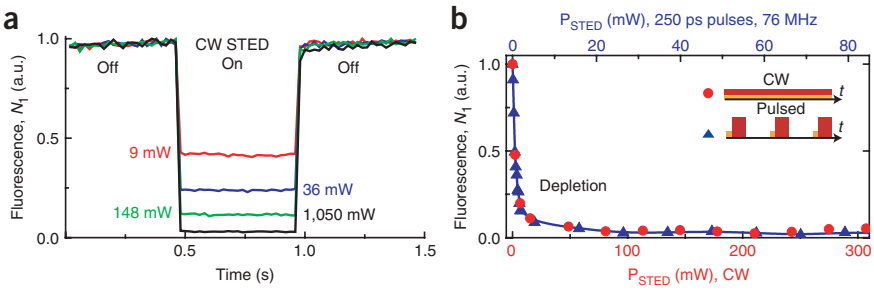

Figure 1 | STED with a CW laser beam focused by a 1.4 NA lens. (**a**) Upon CW excitation at 635 nm, turning on a CW beam at 760 nm for stimulated emission inhibited the fluorescence from an aqueous solution of Atto647N. The fluorescence reflecting the excited state population N_1 decreased with the power of the STED beam as indicated, but instantly recovered with the interruption of the STED beam; minor fluorescence generated just by the STED beam was subtracted. (**b**) Depletion of the fluorescence as a function of the STED beam power P, measured with crimson fluorescent beads excited at 635 nm. Measurements in the CW mode coincide with those in the pulsed mode using 80-ps pulses for excitation and 250-ps pulses for depletion. In the CW mode, the power was 3.6 times larger than the time-averaged power in the pulsed mode. The fluorescence level and hence N_1 follow a function of the form $(1 + \gamma P)^{-1}$, with γ denoting a fluorophore-characteristic constant.

[1]Max Planck Institute for Biophysical Chemistry, Department of NanoBiophotonics, Am Fassberg 11, 37077 Göttingen, Germany. [2]These authors contributed equally to this work. Correspondence should be addressed to S.W.H. (shell@gwdg.de).

RECEIVED 1 AUGUST; ACCEPTED 18 SEPTEMBER; PUBLISHED ONLINE 21 OCTOBER 2007; DOI:10.1038/NMETH1108

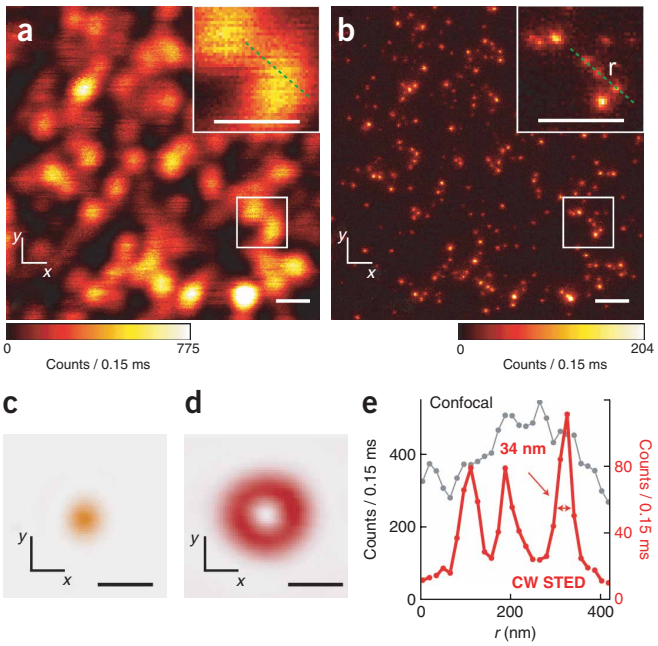

Figure 2 | Nanoscale imaging with CW STED. (**a**,**b**) Raw data of confocal (**a**) and corresponding CW-STED (**b**) image of fluorescent 20-nm-diameter beads. The images were recorded simultaneously with an excitation power of 11 μW (at 635 nm) at the sample and by turning the STED laser (825 mW, 730 nm) on and off line by line. Insets, magnification of the boxed area. Scale bars, 500 nm. (**c**,**d**) The measured focal spot of the excitation light (**c**) along with the measured focal STED doughnut exhibiting a minimum of 250 nm (FWHM; **d**). (**e**) The profile along the dashed line in **a** and **b** exhibits a spot size of 34 nm, indicating an effective resolution of ~29 nm.

area[5]. As many fluorophores[8] have $\sigma \geq 3 \times 10^{-17}$ cm^2 and $\tau_{fl} \approx 3$ ns, P_s typically amounts to 10 mW. Applying a greater power P squeezes the spot diameter (full-width-half-maximum; FWHM) to subdiffraction dimensions following a square-root law[6] $d \approx \lambda_{exc} / (2\text{NA}\ (1 + P/P_s)^{1/2})$.

Notably, P_s is only 3–5 times larger than the time-averaged power reported in experiments with Ti:sapphire–based 250 ps pulsed systems operating at 76 MHz[7]. This is readily understood when envisioning the STED pulse being gradually spread out from the time point of the excitation pulse onward. Stretching it up to about $\tau_{fl} \approx 3$ ns reduces the peak intensity I by about 12-fold but leaves the STED efficiency largely intact because when acting well within the time span τ_{fl}, only the amount of photons in the pulse matters, as STED is a one-photon process. Spreading the pulse further out in time, up to the next excitation pulse arriving after $\tau_{rep} = 1 / (76\ \text{MHz}) = 13.15$ ns unduly reduces I. Hence, to maintain the I continually, as is inherently required for CW operation, the beam power has to be enlarged by a factor of $\tau_{rep}/\tau_{fl} \approx 4$.

To validate this reasoning, we co-aligned the beam of a CW laser diode (FiberTEC635; AMS Technology) delivering $\lambda_{exc} = 635$ nm with that of a Ti:sapphire laser (Mira 900F; Coherent) operating in the CW mode, to be used at $\lambda_{STED} = 760$ nm (see **Supplementary Note** online). We focused the beams into an aqueous solution of the fluorophore Atto647N (Atto-tec) using an oil immersion lens of NA = 1.4 and directed the fluorescence collected by the lens to a point detector. Transiently switching the CW STED beam on and off promptly modulated the fluorescence (**Fig. 1a**). In particular, $P = 9$ mW of CW light reduced the fluorescence by half, in good agreement with our assessment.

Next we compared the CW mode with the standard pulsed mode by converting the Ti:sapphire laser into the mode-locked (pulsed) mode and applying a pulsed 635 nm diode (Picoquant) for excitation. The key phenomenon in both cases is the saturated

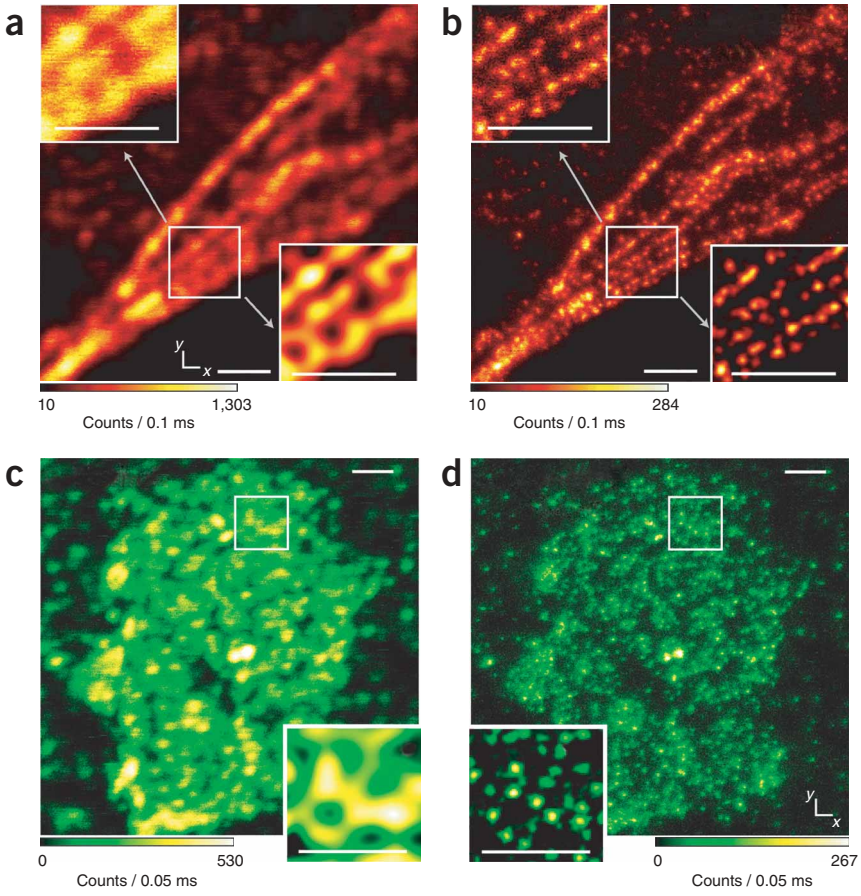

Figure 3 | Immunofluorescence CW STED microscopy shown in a side-by-side comparison with confocal microscopy. (**a**,**b**) Confocal (**a**) and CW-STED (at 750 nm; **b**) micrographs of neurofilaments in human neuroblastoma marked by the red emitting dye Atto647N. Insets, magnified view of the raw data in the boxed areas (top left), the same data after a linear deconvolution (bottom right). (**c**,**d**) Confocal (**c**) and CW-STED (at 647 nm; **d**) micrographs of syntaxin clusters in a cell membrane, immunostained an antibody conjugated with the dye Atto565. Insets show the data in the corresponding boxed areas after a linear deconvolution. Scale bars, 1 μm.

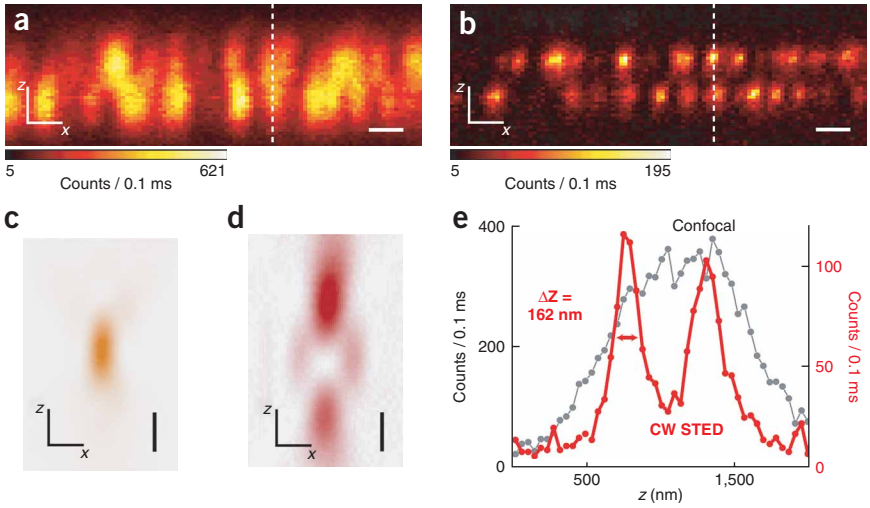

Figure 4 | 3D superresolution in axial optical sections (*x*-*z* images). (**a**–**d**) Confocal (**a**) and CW-STED (**b**) images of bead clusters recorded with the excitation spot (**c**) overlapped by an axial STED doughnut (**d**) improving the resolution primarily along the optic axis (*z*), but also in the focal plane (*x*,*y*). Scale bars, 500 nm. (**e**) Intensity profiles along the *z* axis extracted from images in **a** and **b** at the dashed lines, quantifying the axial resolution gain in CW STED over confocal microscopy with this doughnut.

depletion of the S_1 with increasing power P. In both modes of operation, we collected data for crimson fluorescent beads (Invitrogen) featuring an emission peak at 645 nm and a fluorescence lifetime τ_{fl} = 3.77 ns (**Fig. 1b**). The fluorescence depletion increased for greater STED intensities, in agreement with $N = k_{exc} / (k_{exc} + k_{fl} + \sigma P)$; fluorescence depletion was virtually identical for the pulsed and the CW STED mode. The only difference was that the power of the CW beam was ~3.6 times larger than the time-averaged power of the STED pulses, in agreement with our calculation τ_{rep}/τ_{fl} = 13.15 ns / 3.77 ns = 3.5.

The saturated depletion observed in the images in **Figure 1b** suggests that conversion of the CW STED beam into a doughnut[3,5–7] should yield subdiffraction focal plane resolution. In a CW-STED image of 20 nm crimson fluorescent beads, recorded with P = 812 mW, images of isolated beads displayed an average FWHM of 34 nm (**Fig. 2**). Considering the bead diameter yields an effective lateral resolution $d \approx$ 29 nm—that is, a resolution increase of eightfold in all directions in the focal plane. Application of 161 mW gave $d \approx$ 61 nm, that is, a fourfold increase. This increase in resolution is entirely physical, requiring no mathematical processing.

We compared the images of the heavy subunit of neurofilaments in a fixed human neuroblastoma cell[9], immunologically labeled with an antibody conjugated to Atto647N (**Fig. 3a**,**b**). The CW excitation power was 6.7 μW at 635 nm. Contrary to the confocal image, the CW STED image (P = 423 mW at 750 nm) exhibited a substructure of separated spots in the axon. To quantify the resolution in the sample, we also imaged isolated antibodies, which because of their small size directly gave the lateral resolution. We found $d \approx$ 230 nm for the confocal and $d \approx$ 52 nm for the CW STED mode. We imaged the protein syntaxin on a membrane sheet of a fixed mammalian (PC12) cell[10] (**Fig. 3c**,**d**). In this case, the secondary antibody was coupled with the yellow-orange emitting dye Atto565 that can be effectively excited with 25 μW of a common 532 nm laser diode. We performed CW STED with the widely used 647 nm line of a krypton laser (Innova; Coherent). Measurements with isolated antibodies showed that with this dye-wavelength pair, P = 114 mW sufficed to attain $d \approx$ 61 nm. Using CW STED we detected individual protein clusters that are blurred in the confocal image (**Fig. 3d**).

The viability of CW STED with two different dye-wavelength pairs shows that CW-STED microscopy with at least two color channels is possible. The fact that Atto565 requires a nearly 4 times lower P than Atto647N implies a larger σ of Atto565 at the applied λ_{STED}. It also proves that the best strategy to avoid exceedingly large P is to match the dye to λ_{STED}.

The need for greater power in the CW STED mode must not be attributed to an inherently less efficient use of photons; stimulated

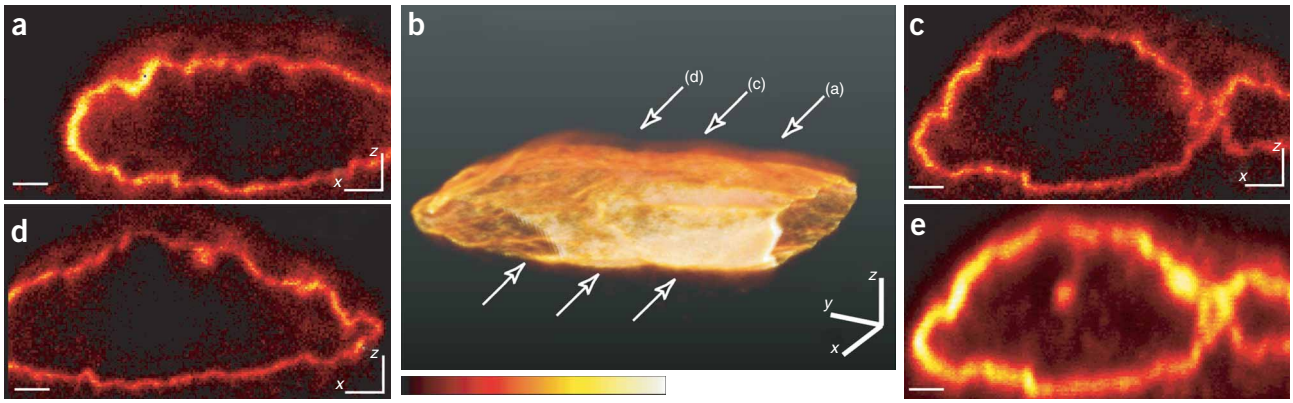

Figure 5 | The 3D subdiffraction-resolution recording of the nuclear lamina of a fixed mammalian cell (immunofluorescence labeling) using the CW STED doughnut of **Figure 4d**. (**a**–**d**) Three *x*-*z* CW STED images of a 3D data stack consisting of 200 individual *x*-*z* images (**a**,**c**,**d**). A surface rendered view of the 3D data stack, reproducing the nuclear lamina as an 'empty bag' (**b**). The arrows indicate the positions of the *x*-*z* sections shown in **a**,**c**,**d**. (**e**) Confocal image counterpart to **c**. Scale bars, 1 μm.

emission is a one-photon process. The requirement for a greater (average) power is because the dye is continually illuminated. For the same reason, CW operation has the potential to deliver a slightly larger instant fluorescence flux, which will be of great value for fast STED imaging. In fact, the 52-nm resolution images (**Fig. 3**) exhibit up to 280 photon counts per 100 µs, per 15-nm pixel, indicating that, at least for these dyes, photobleaching by the CW beam is not prohibitive, and that many photons can be collected in a CW STED system. Although we recorded these images with a slow stage-scanning system, spreading out the photon counts over several recordings through repetitive scanning is possible. In fact, we verified this by recording consecutive STED images of immunologically labeled protein distributions (**Supplementary Note**).

Moreover, we recorded 3D image stacks and demonstrated the ability of CW STED microscopy to break the diffraction barrier along the *z* axis as well (**Fig. 4**). To this end we implemented the 'doughnut' (STED-PSF; **Fig. 4d**), which by featuring a strong intensity maximum above and below the focal plane compresses the spot along the *z* axis[3]. This doughnut also features a ring-shaped component squeezing the fluorescent spot in the lateral direction. At the applied $\lambda_{STED} = 750$ nm, the axial and lateral FWHM values of the doughnut minimum were ~740 nm and 350 nm, respectively.

The simultaneous gain in *x*, *y* and *z* resolution is evidenced in the side-by side comparison of a CW STED with a confocal reference *x*-*z* image of two axially separated layers of 40-nm-diameter crimson fluorescent beads with its CW STED counterpart. Although the confocal recording does not resolve the beads, the corresponding STED image clearly separates them. The axial resolution provided by CW STED is ~170 nm (FWHM), which is 3.5 times greater than that of a confocal microscope. The gain in lateral resolution is not as pronounced as with the previous doughnut, as the lateral FWHM of the central minimum is 40% greater. Also the intensity at the doughnut crest is lower with respect to the peak maximum. Nonetheless, the focal plane resolution is almost doubled, from 250 nm to 139 nm.

Next we applied this far-field 3D superresolution by CW STED to record the nuclear lamina of a mammalian cell in 3D, immunologically labeled with an antibody conjugated with Atto647N. We collected a stack of 200 *x*-*z* subdiffraction images separated by 60 nm in the *y* direction and generated a surface-rendered 3D representation of the nuclear lamina (**Fig. 5**). The pixel size in the *x* and *z* direction was 60 and 70 nm, respectively. At $\lambda_{STED} = 750$ nm we obtained an axial resolution of ~200 nm, which resulted in considerably improved *x*-*z* sections as compared to the confocal recording. The ability to record 3D stacks at this pixilation underscores that the CW version of STED microscopy is not generally prohibited by photobleaching. On the contrary, the CW STED approach can provide subdiffraction resolution in all directions.

CW STED should be difficult with dyes featuring a substantial dark (triplet) state built-up because CW illumination will promote bleaching through dark state excitation[5,11]. Applying a dark state relaxation (D-Rex) illumination scheme in which pairs of synchronized pulses are used featuring an interpulse break greater than the ~1 µs lifetime of these states will remain mandatory for those dyes[5,11]. For a given resolution, for example, $d = 50$ nm, the D-Rex scheme will gather more photons from the dye molecule. Attaining $d < 30$ nm should also be more difficult with CW operation, unless dye-wavelength combinations with larger σ are identified.

An important insight is that the intensity I of the CW beam is lower by $\tau_{fl}/250$ ps $\approx$ 10–15-fold than the peak intensity of the 250 ps STED pulses used until now. As photodamage mechanisms[12] usually scale with I^m, with $m \geq 2$, the reduction of I by 10–15-fold is co-responsible for the comparatively large photon flux obtained in our recordings. The lower I also reduces undesired multiphoton excitation of fluorophores from the S_0. Therefore, the CW experiments reported herein also imply that STED pulses of $\sim\tau_{fl}$ duration should improve the performance of (D-Rex) STED microscopy in general.

The motivation for pulses in STED was the temporal separation between excitation and de-excitation, and the low time-averaged power resulting from the interpulse breaks. These advantages do not generally outweigh those brought about by simple CW illumination. Temporal separation between excitation and STED is not crucial as long as $k_{exc} \ll k_{STED}$. With three fluorophores having met the CW STED conditions, more applicable dyes will be available once other laser wavelengths are explored. Special attention is now being directed also to the wavelengths provided by CW semiconductor lasers. The viability of CW illumination greatly expands the range of STED microscopy operation. Finally, our results demonstrate that adding a bright, doughnut-shaped CW beam for STED converts a regular scanning (confocal) fluorescence microscope[13] into a microscope with nanoscale resolving power both in the focal plane and along the optic axis.

Note: Supplementary information is available on the Nature Methods website.

ACKNOWLEDGMENTS

We thank B. Hein for sharing the setup, T. Lang (Department of Neurobiology) for providing the PC12 membrane sheets, A. Schönle, V. Westphal and J. Keller for help with the measurement and analysis software, and B. Rankin for critical reading of the manuscript.

Published online at http://www.nature.com/naturemethods
Reprints and permissions information is available online at http://npg.nature.com/reprintsandpermissions

1. Abbe, E. *Arch. Mikr. Anat.* **9**, 413–420 (1873).
2. Hell, S.W. & Wichmann, J. *Opt. Lett.* **19**, 780–782 (1994).
3. Klar, T.A., Jakobs, S., Dyba, M., Egner, A. & Hell, S.W. *Proc. Natl. Acad. Sci. USA* **97**, 8206–8210 (2000).
4. Willig, K.I., Rizzoli, S.O., Westphal, V., Jahn, R. & Hell, S.W. *Nature* **440**, 935–939 (2006).
5. Donnert, G. *et al. Proc. Natl. Acad. Sci. USA* **103**, 11440–11445 (2006).
6. Westphal, V. & Hell, S.W. *Phys. Rev. Lett.* **94**, 143903 (2005).
7. Willig, K.I. *et al. Nat. Methods* **3**, 721–723 (2006).
8. Lakowicz, J.R. *Principles of Fluorescence Spectroscopy* (Plenum Press, New York, 1983).
9. Yuan, A., Nixon, R.A. & Rao, M.V. *Neurosci. Lett.* **393**, 264–268 (2006).
10. Sieber, J.J. *et al. Science* **317**, 1072–1076 (2007).
11. Donnert, G., Eggeling, C. & Hell, S.W. *Nat. Methods* **4**, 81–86 (2007).
12. Hopt, A. & Neher, E. *Biophys. J.* **80**, 2029–2036 (2001).
13. Pawley, J.B. (ed.). *Handbook of Biological Confocal Microscopy* (Springer, New York, 2006).